

Characterization and Consideration of Topological Impact of Wireless Propagation in a Commercial Aircraft Environment

Erik Aguirre, Peio López, Leire Azpilicueta, Javier Arpón and Francisco Falcone

Electrical and Electronic Engineering Department, UPNA, Pamplona, Navarra, Spain

Abstract: Wireless systems are gaining a relevant role for multiple communication tasks within commercial aircrafts. In this work, wireless propagation in an indoor commercial airplane cabin will be analyzed. The impact of indoor elements, such as passenger seats, luggage compartments and a dual deck structure will be considered, with the aid of in-house implemented 3D ray launching code. Multipath propagation plays a relevant role, given by the time domain characteristics obtained by spatially dependent power delay profiles and delay spread. The use of deterministic techniques in order to consider the inherent complexity of the airplane cabin can aid in wireless system planning in order to increase overall system capacity whilst reducing power consumption.

Key Words: Aircraft Cabin, 3D Ray Launching, Power Delay Profiles, Delay Spread

1. Introduction

Since the minimization of aircraft weight became a priority in order to gain capabilities and reduce fuel consumption, there has been an increasing interest on using wireless communication systems onboard, in order to replace existing cable connections. Besides, wireless technologies provide easier and cheaper system maintenance, deployment and upgrade whilst reduction in life-cycle cost is obtained. In addition, the probability of arc faults is reduced by eliminating some of the signal lines.

Due to the mentioned advantages of wireless technologies, aircraft manufacturers as well as research groups have shown strong interest in development of wireless systems for onboard use. These systems can be implemented for applications outside the aircraft, e.g. GPS landing systems [1], communications with satellites [2], wildlife research [3], remote sensing applications [4], data transfer within air vehicles [5], air-to-air communications [6], radar [7] and sensing [8], among others. Focusing in aeronautic transportation sector, there are also applications within the cabin, e.g. wireless multimedia networks for in-flight entertainment [9-10], deployment of Wireless Local Area Network (WLAN) communication systems [11-12], pilot health monitoring by means of Wireless Sensor Networks (WSN) [13], military [14] and sensing and monitoring [8, 15]. As it can be seen, there is a wide range of wireless

technologies which are used for a broad range of applications, with different systems employed depending on the final intended use. The main wireless technologies used are WiFi, ZigBee, Bluetooth, RFID, 60 GHz mm-wave systems, Ultra Wide Band (UWB) and energy harvesting systems, such as EnOcean. It is important to note the potential use of these systems due to the fact that there is a possibility of interfering with other wireless devices. Therefore unlicensed bands are excluded from applications related to safety, as the landing and taking off systems. Related to this, there is concern about the proliferation of portable electronic devices (PED) and the interference with airplane electronic systems that might be created [16].

Therefore, an aircraft, especially the interior portion, is a complex environment which requires an in-depth radiopropagation analysis. The behavior of the radio channel in indoor scenarios is not a trivial issue [17-18] and depends heavily on the complexity of the environment. The appearance of degradation effects is due fundamentally to multipath components, but also phenomena like reflection, refraction, diffraction and scattering proves the study of the radio channel to be a complex task [19].

Several works can be found in the literature addressing wireless channel characterization within an aircraft cabin. Some of them are focused on optical wireless networks [20-24], but most of them address the radio channel. For propagation estimations and characterization of the radio channel within the aircraft cabin, different wireless technologies and simulation methods have been used in the literature. Initially the statistical characterization of the radio channel performing measurements within the scenario [25-29], including MIMO systems [30-31] has been obtained. Other approaches do not need a measurement campaign to obtain a model for the radio channel and power distribution within the aircraft cabin. In this case, different simulation methods have been presented in the literature, as the integral equation (IE) – multiple image theory (MIT) hybrid technique [32], fuzzy logic [33], neural network approach [34] and commercially available software code [35-36]. These methods usually define a simple radio channel in a simple aircraft cabin model. The deterministic Finite Difference Time Domain (FDTD) method improves strongly the accuracy and precision of the simulation results, obtaining reliable estimations of the propagation within a more complex aircraft model (with seats, seats, persons, etc.), since it is based on numerical approaches to the resolution of Maxwell's equations [37-38]. But it is highly time consuming due to inherent computational complexity when large scenarios are simulated. It is necessary therefore to apply alternative simulation methods to finally obtain estimations in a reasonable way. Offering this reasonable trade-off between precision and required calculation time, there are the ray tracing and ray launching methods based on Geometrical Optics (GO) and Geometrical Theory of Diffraction (GTD) [39]. For these reason, ray tracing is the most widely used method for simulating the electromagnetic propagation within an aircraft cabin [40-50].

In this paper, the simulation of the cabin of an Airbus A380 by means of an in-house ray tracing method is presented. The ray tracing algorithm has been developed in the Public University of Navarre and has been validated in previous works, where the radiopropagation within indoor complex scenarios has been studied [51-54]. In this work the Airbus A380 cabin is simulated, which is divided in two 50-meter decks, making it the largest commercial aircraft in the world since it was built in the middle of the last decade. The accurate results obtained with the in-house ray tracing method are determined by the complexity of the cabin modeling as well as the parameters that can be set for the simulations (e.g. antenna type, radiation pattern, transmitted power level, scenario cuboids size, etc.). While many of the cabin models used in the literature have a simple structure, here a full detailed cabin is presented, as shown later in this work. The shape and size of all the elements and obstacles within the scenario have been defined according to the real dimensions, as well as their material parameters (dispersive dielectric constant and loss tangent), which are relevant in order to calculate an accurate estimation of the electromagnetic propagation and the phenomena associated to it (diffraction, reflection and refraction). When ray tracing technique is used for the simulation of an aircraft main cabin, typically the technologies studied are WiFi (IEEE 802.11) and UMTS [40-50]: 2.4 GHz and 5 GHz frequency bands for WiFi, and 1900 MHz and 2100 MHz bands for UMTS. The 900 MHz band has only been used for a MIMO system analysis [45], but the simulated aircraft cabin is simple in this case.

In this work, an in-depth propagation study is presented for 2.4 GHz (which can also be considered to create an onboard ZigBee-IEEE 801.15.4 network [55]), 5 GHz and 900 MHz within a detailed large aircraft scenario by means of an in-house 3D ray tracing algorithm, showing power distribution planes and time domain results, as power delay profiles (PDP) and delay spread. The differences between an empty cabin and the cabin with seats are also shown, in order to show the relevance of material absorption and strong multipath components in the full scenario.

2. Ray Launching Technique and Simulation Scenario

In order to assess the impact of the morphology and topology inside the airplane, it is highly important to consider an adequate radio planning method. In this work, an in-house developed 3D Ray launching algorithm has been implemented in order to verify that the variability and the topology of the environment affect the electromagnetic propagation [51-53]. Ray launching techniques are based on identifying a single point on the wave front of the radiated wave with a ray that propagates along the space following a combination of optic and electromagnetic theories. Each ray propagates in the space as a single optic ray. The principle of the ray launching method is based on Geometrical Optics (GO) and Uniform Geometrical

Theory of Diffraction (UTD). Rays are launched from the transmitter at an elevation angle θ and with an azimuth angle Φ , as defined in the usual coordinate system. They propagate along the space interacting with obstacles, causing physical phenomena such as reflection, refraction and diffraction, as it is shown in Fig. 1.

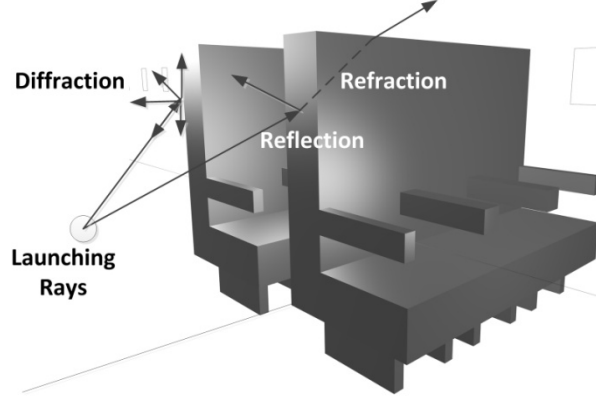


Fig. 1. Principle of operation of the in-house developed 3D Ray Launching Algorithm.

The number of rays considered and the distance from the transmitter to the receiver location determines the available spatial resolution and, hence, the accuracy of the model. It is important to emphasize that a grid is defined in the space to save the parameters of each ray. Thus, the parameters of these rays are stored as they enter to each hexahedral until the ray has a certain number of reflections or it has exceeded the pre-propagation time set. The algorithm works in an iterative manner, considering a ray and its reflections, storing the created ray for processing later the phenomenon of diffraction. Parameters such as frequency of operation, number of multipath reflections, separation angle between rays, and cuboids dimension are introduced. The radiation patterns of the transmitter and receiver antenna are also taking into account in the algorithm. The received power is calculated at each point considering the dispersive materials within the scenario, taking into account the dielectric constant and permittivity at the frequency range of operation for each obstacle and through the medium.

The coefficients for the vertical and horizontal polarization for the reflected and transmitted rays are given by the Snell's law [56] by

$$T^{\perp} = \frac{E_t^{\perp}}{E_i^{\perp}} = \frac{2\eta_2 \cos(\Psi_i)}{\eta_2 \cos(\Psi_i) + \eta_1 \cos(\Psi_t)} \quad (1)$$

$$R^{\perp} = \frac{E_r^{\perp}}{E_i^{\perp}} = \frac{\eta_2 \cos(\Psi_i) - \eta_1 \cos(\Psi_t)}{\eta_2 \cos(\Psi_i) + \eta_1 \cos(\Psi_t)} \quad (2)$$

$$R^{\parallel} = \frac{E_r^{\parallel}}{E_i^{\parallel}} = \frac{\eta_1 \cos(\Psi_i) - \eta_2 \cos(\Psi_t)}{\eta_1 \cos(\Psi_i) + \eta_2 \cos(\Psi_t)} \quad (3)$$

$$T^{\parallel} = \frac{E_t^{\parallel}}{E_i^{\parallel}} = \frac{2\eta_2 \cos(\Psi_i)}{\eta_1 \cos(\Psi_i) + \eta_2 \cos(\Psi_t)} \quad (4)$$

where $\eta_1 = 120\pi/\sqrt{\varepsilon_{r1}}$, $\eta_2 = 120\pi/\sqrt{\varepsilon_{r2}}$ and Ψ_i, Ψ_r and Ψ_t are the incident, reflected and transmitted angles respectively.

Once the parameters of transmission T and reflection R are calculated, and the angle of incidence Ψ_i and Ψ_t , the new angles (θ_r, ϕ_r) of the reflected wave and (θ_t, ϕ_t) of the transmitted wave can be calculated.

The diffracted field is calculated by [57]

$$E_{UTD} = e_0 \frac{e^{-jks_1}}{s_1} D^{\perp\parallel} \sqrt{\frac{s_1}{s_2(s_1 + s_2)}} e^{-jks_2}, \quad (3)$$

where s_1, s_2 are the distances represented in Fig. 2, from the source to the edge and from the edge to the receiver point.

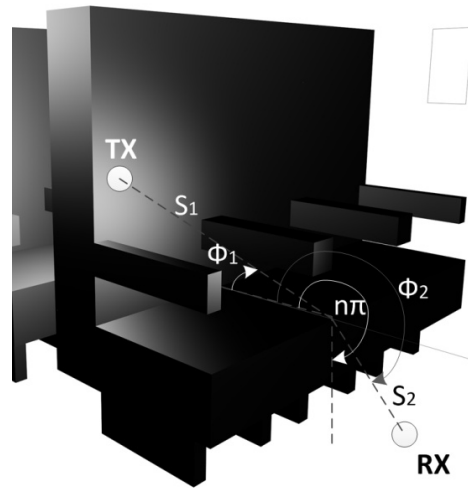


Figure 2 Geometry for wedge diffraction coefficients

A full detailed Airbus A380 commercial aircraft model has been implemented for this work, considering all its characteristics, including two floors with more than 500 seats (taking in account their position depending on class distribution within the aircraft), bathrooms, luggage compartments and windows. Realistic dimensions for the cabin and seats have been implemented programming 49.9 m X 6.58 m X 4.6 m scenario divided in 49.9 m X 6.58 m X 2.3 m decks including also stairs between two decks (Fig. 3). A typical A380 distribution has been chosen for the position of all items inside the aircraft, e.g. in first floor four groups of seats can be distinguished, first class with higher space between seats in the beginning of the plane, a group of second class seats

in the following section and two sections in the last part of the aircraft for tourist class, a total number of 334 seats for first floor and 216 for second tier.

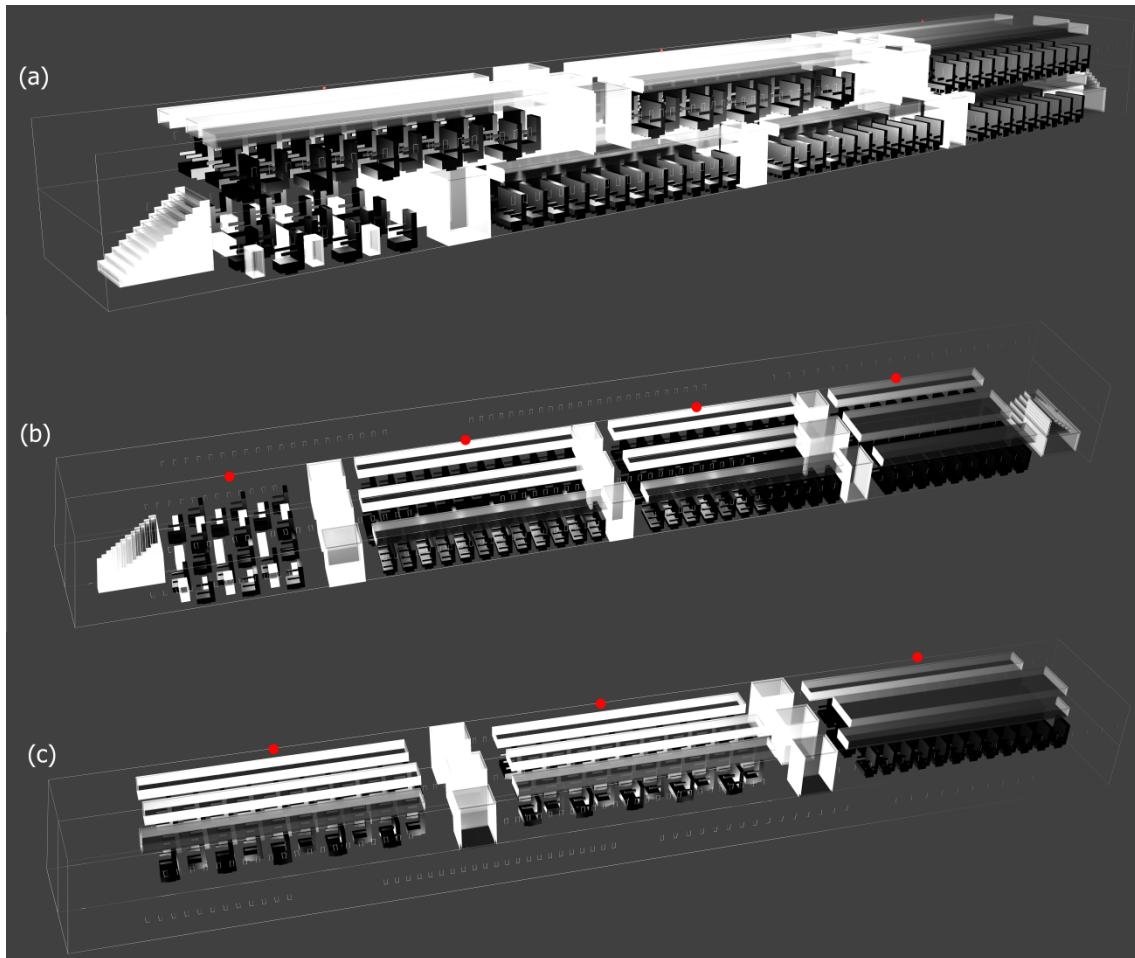


Figure 3 3D Representation of simulated scenario showing complete A380 aircraft (a) and the detail of first (b) and second floor (c).

One of the goals of this work is to consider the influence of the topology and morphology of the elements inside the aircraft cabin. Therefore two kinds of scenarios have been programmed: an airplane cabin with all seats (Full aircraft) and on the other hand an airplane without seats (Empty aircraft). This scenarios have been sub-divided in a mesh with 2.500.000 cuboids of 0.099m X 0,13m X 0.046m dimensions.

In order to obtain coverage throughout the airplane considering a real communications system, seven antennas have been distributed inside the aircraft (Depicted as red points in Fig. 3) in a distance of 10cm to the left wall and ceiling, three in the first floor and four in the second floor emitting all of them with quarter-sphere shape radiation pattern (Fig. 4) in three different frequencies, 900MHz, 2.4 GHz and 5GHz .

Ray Launching Simulation Parameters	
Frequency	900 MHz/2.4 GHz/5 GHz
Transmitter Power	27 dBm
Reflections	6
Vertical plane angle resolution $\Delta\theta$	1°
Horizontal plane angle resolution $\Delta\varphi$	1°

Table 1 Simulation Parameters Employed in the Analysis

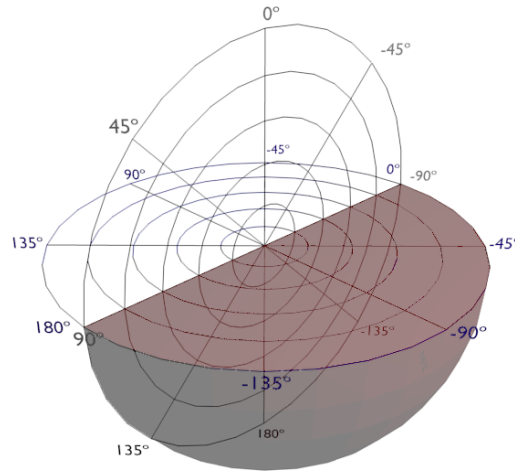


Figure 4 Radiation pattern of the seven transmitting antennas configured inside the scenario.

3. Statistical analysis

In order to check the proper operation of developed code within the aircraft cabin, the statistical analysis of the one antenna scenario is presented in this section.

Path loss (PL) is defined as the ratio of the effective transmitted power to the received power:

$$PL(dB) = P_T(dBm) + G_T(dBi) + G_R(dBi) - P_R(dBm), \quad (0.1)$$

Where P_T , P_R , G_T and G_R denote de transmitted power, the received power, the transmitter antenna gain and the receiver antenna gain, respectively.

According to the literature, the modeling method for Path Loss inside the complex environment of an aircraft is the empirical model of log-distance [25], expressed as follows:

$$PL(d) = PL_0 + 10n \log_{10}(d) + X_\sigma \quad (0.2)$$

Where PL_0 is the intercept, d is the Tx-Rx separation distance in meters, and n is the PL exponent dependent on the specific propagation environment indicating the rate at which PL

increases with distance. In free space propagation, n equals 2. X_σ denotes shadow fading with standard deviation σ .

Fig 5 shows the scatter plot of the simulated values path loss for a height of 0.92m with respect to the transmitter-receiver separation in logarithmic scale. Additionally, the linear regression line, resulting from a minimum mean square error (MMSE) analysis, is shown. The corresponding path loss exponent is $n=0.98$ with a standard deviation of $\sigma=11.6$. Accordingly, n is quite smaller than for free space propagation. This is due to the multipath components which are really rich and significant; hence energy decreases slowly within the indoor environment. The value of n lies in the range of values found for indoor radio wave propagation in complex environments [25, 58].

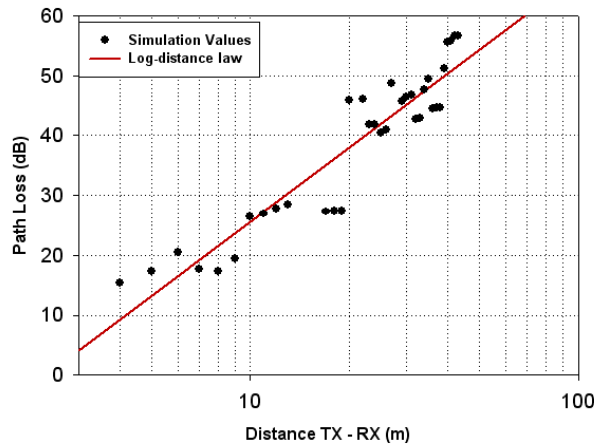


Fig. 5. Path loss versus Tx-Rx separation with linear regression fit.

As stated previously, in an indoor environment the median value of the signal strength is monotonous decreasing with distance. The median level is subject to two major variations. One is large-scale signal variations, which it has been found to be normally distributed [59], as it is previously shown in Fig. 5. The second variation is the small-scale variation (on the order of tens of wavelengths) due to the vector combination of multiple rays arriving at the local vicinity of the portable communications antenna. The small-scale variation for narrowband signals is distributed according to Rayleigh statistics [59]. An analysis of the small-scale fading within the aircraft has been made. The probability density function (PDF) of a Rayleigh-distributed random variable is given by

$$f(s) = \frac{s}{\sigma^2} e^{-\frac{s^2}{2\sigma^2}} \quad (0.3)$$

Where $f(s)$ is the envelope of the voltage distribution of the signal, and σ^2 represents the average signal power. Fig 6 illustrates that the small-scale variations inside this complex environment lead to a Rayleigh behavior which is typical of the signal statistics encountered in many indoor environments [59].

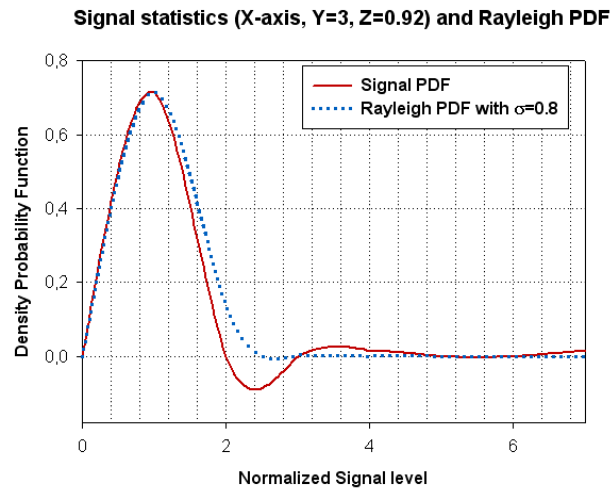


Fig. 6. Signal statistics compared with Rayleigh PDF for height 0.92m.

4. Radioplanning Simulation Analysis Results

Once the simulation scenario has been defined, radioplanning results can be obtained. As it can be seen in Figure. 7 three kinds of cut planes are presented: on one hand vertical cut planes of RF power distribution are represented by XZ planes and on the other hand horizontal cut planes of RF power distribution are represented by XY planes, for first deck or height (H1) and for the second deck or height (H2).

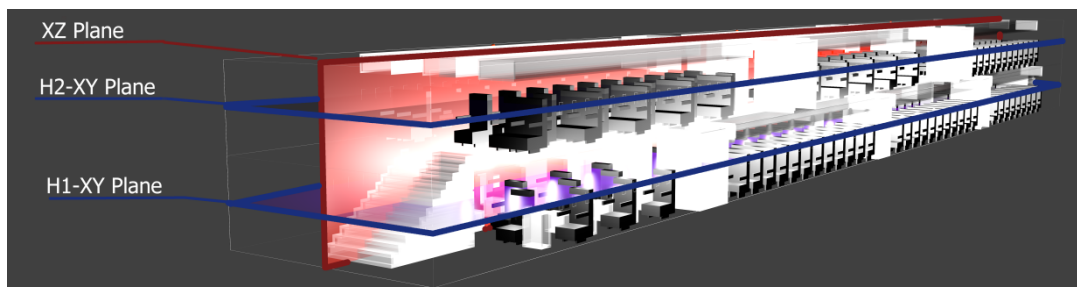


Figure 7 Representation of the cut planes used for obtaining data

The location of radiating elements which represent potential coverage sectors or hotspots play a key role in the operation of the planned systems and hence on the radioplanning election for the final network to be deployed. In Figure 8 XZ planes for 900 MHz and $Y=1.70\text{m}$, $Y=2.29\text{m}$ and $Y=4.68\text{m}$ are depicted. Considering that XY (0,0) point is situated in the right wall of the aircraft and the antennas in the left wall, it can be shown that the highest power levels are in $Y=4.86\text{m}$ plane.

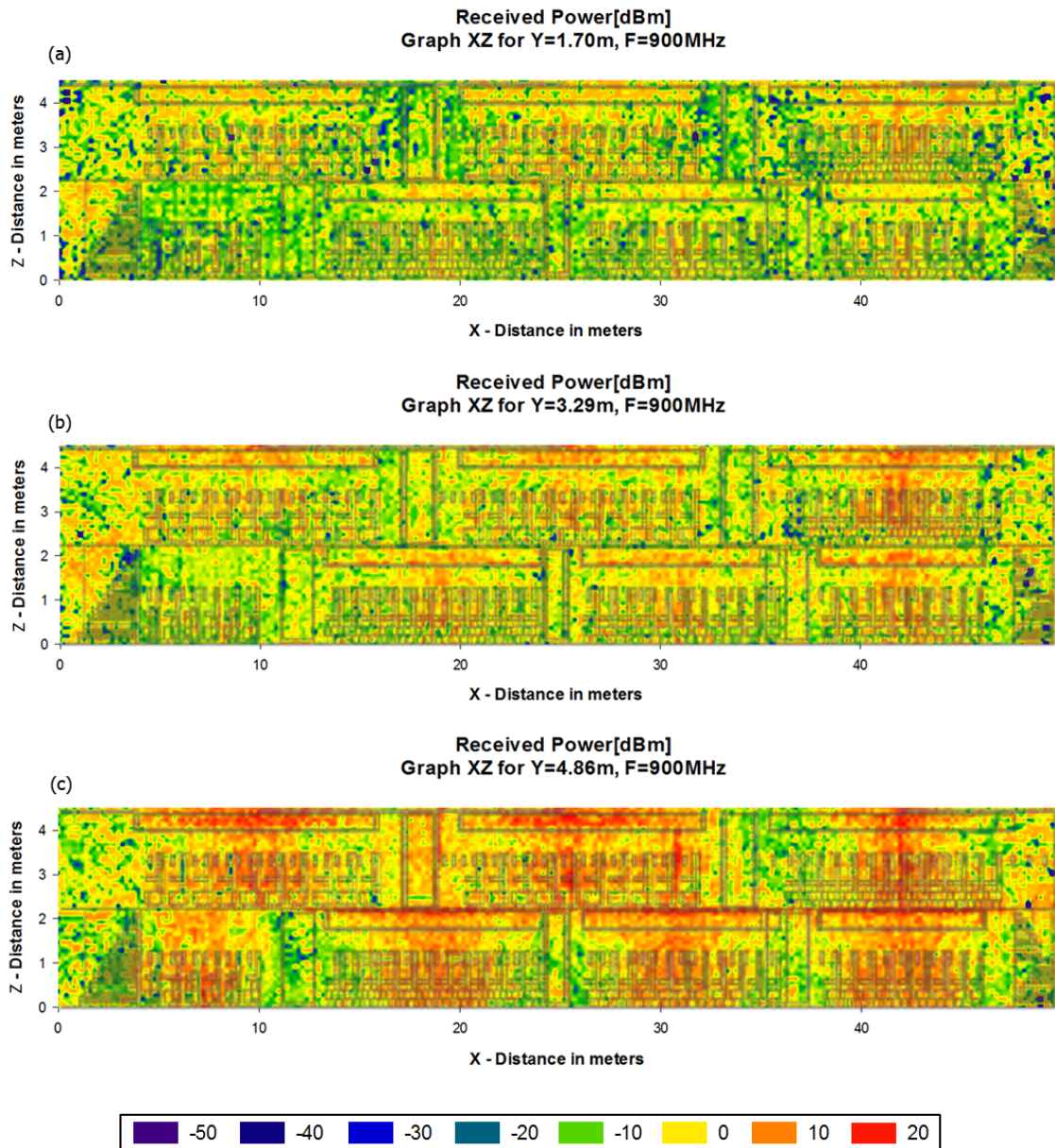


Figure 8 Estimation of received power for three different values of Y and 900 MHz frequency in XZ planes with the aircraft overhead (Full Aircraft).

Due to the fact that commercial communication systems such as WLANs or Wireless Sensor Networks can operate in several frequency bands, radioplanning estimations should be obtained for the eventual frequency allocation to be adopted. Figure 8(b) and Figure 9 present simulation results for radiating elements operating at 900MHz, 2.4GHz and 5GHz, where for the same Y=2.39m XZ plane the power level obtained emitting with 900MHz is higher than for 2.4GHz and both are higher than the power received with 5GHz, as can be expected.

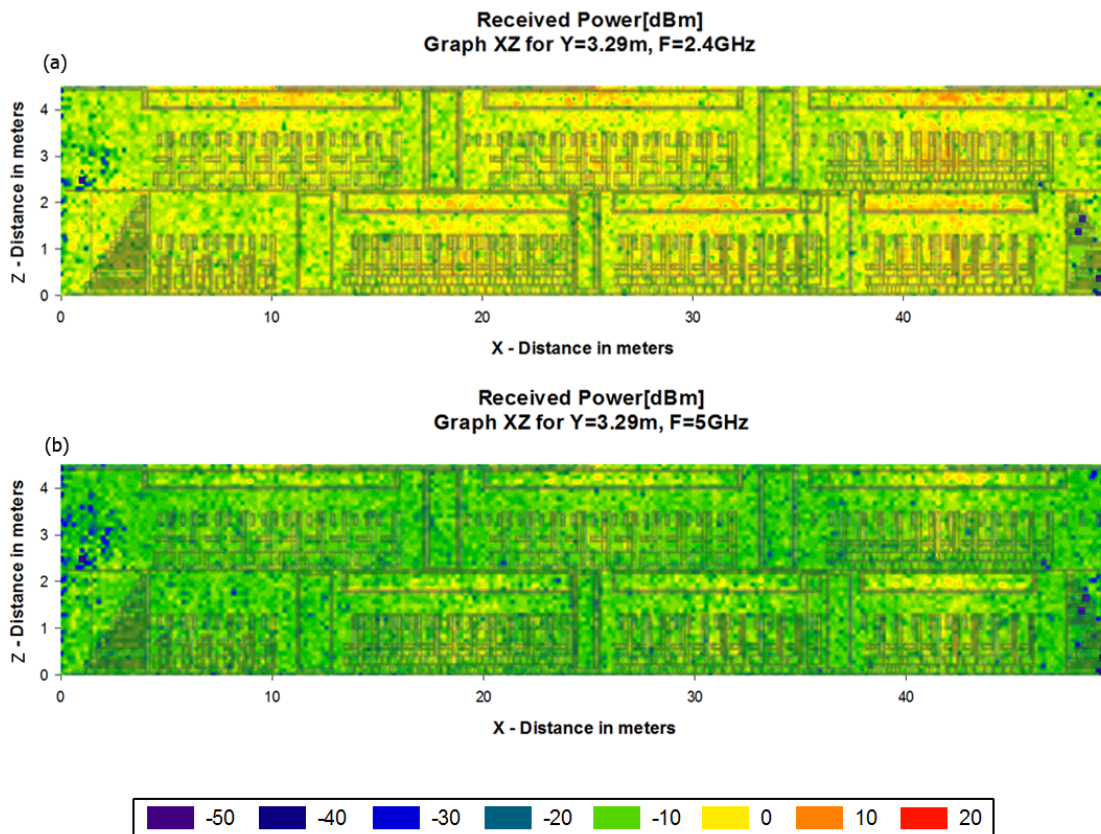


Figure 9 Estimation of received power for 2.4GHz (a) and 5GHz (b) and Y=3.29m in XZ planes with the aircraft overhead (Full Aircraft).

In Figure 10 the empty aircraft scenario is represented in the same conditions as the previous (Y= 2.29m) for 900 MHz operating frequency. Comparing with the second graph of Figure 8 where the airplane is full the difference is visible. In the latter case the level of power is lower, due to the multipath contribution that has been caused by the absence of seats which absorb a substantial amount of the power which is ricocheting in full aircraft causing non negatively coupling.

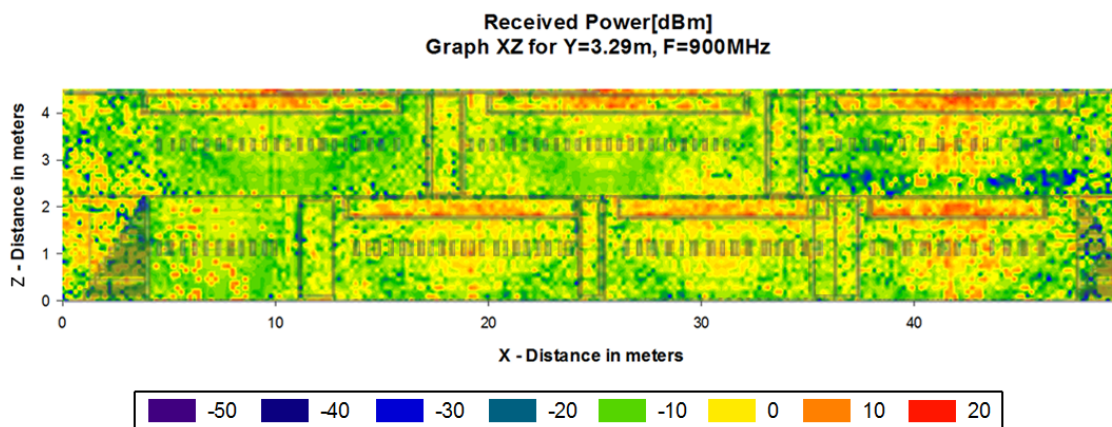


Figure 10 Estimation of received power for 900MHz and Y=3.29m in XZ planes with the aircraft overhead (Empty Aircraft).

This behavior is depicted in Figures 11 and 12 where XY H1 and H2 planes are compared in empty and full aircraft for 900 MHz. Also, distance dependence is visible, bearing in mind that the antennas are located in the left wall, higher power is received in the left side of the aircraft. A low height (0.60m) has been chosen for H1 and H2 so the antenna influence is visible, because in second deck first height and second height antennas power is added and a higher power level is received compared with H1's 0.60m(Figure 8).

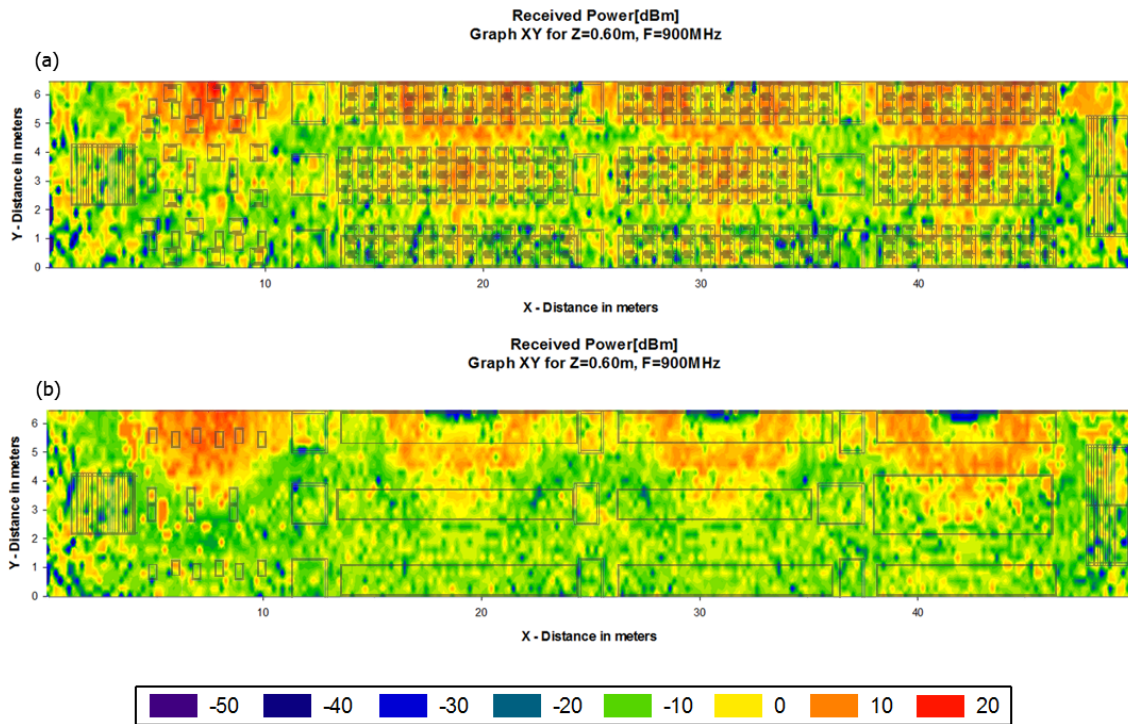


Figure 11 Estimation of received power for 900 MHz and Y=0.60m in XY planes for full (a) and empty (b) aircraft with its picture overhead (H1).

In Figure 13 a comparison between full aircraft and empty aircraft linear distance power distributions for 2.4GHz and 5GHz are depicted. Both the frequency dependence of radiopropagation losses and the difference among full and empty aircraft can be quantitatively seen, receiving more power in the full aircraft scenario and a difference of 5 dB between both operating frequencies.

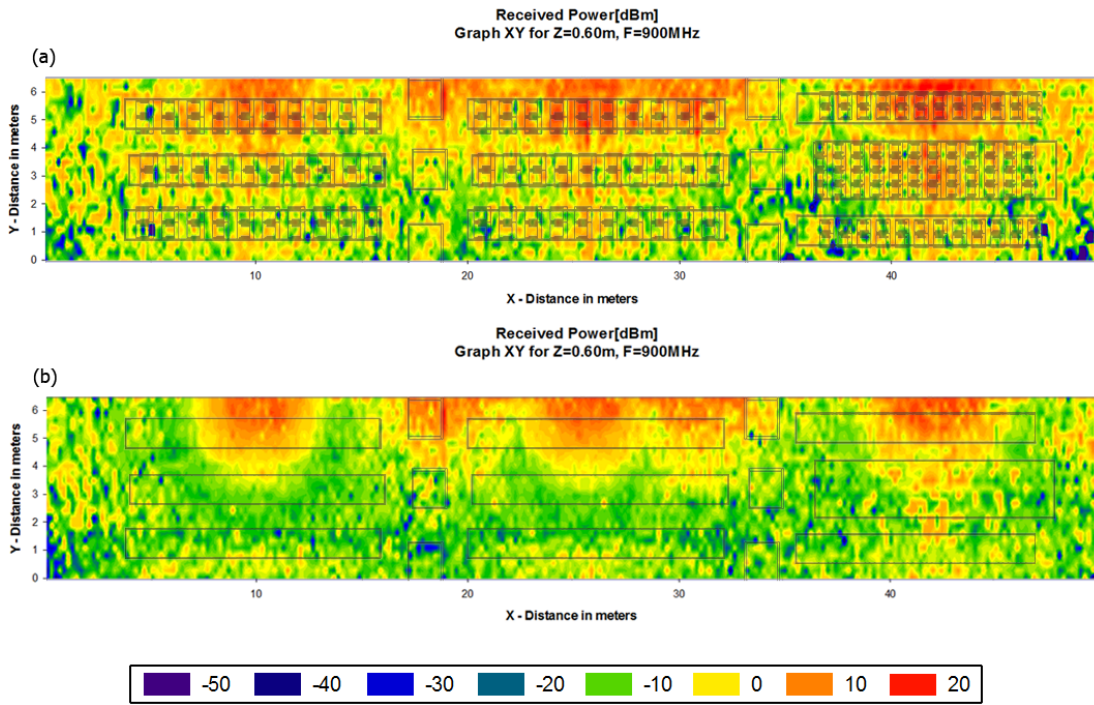


Figure 12 Estimation of received power for 900 MHz and Y=0.60m in XY planes for full (a) and empty (b) aircraft with its picture overhead (H2).

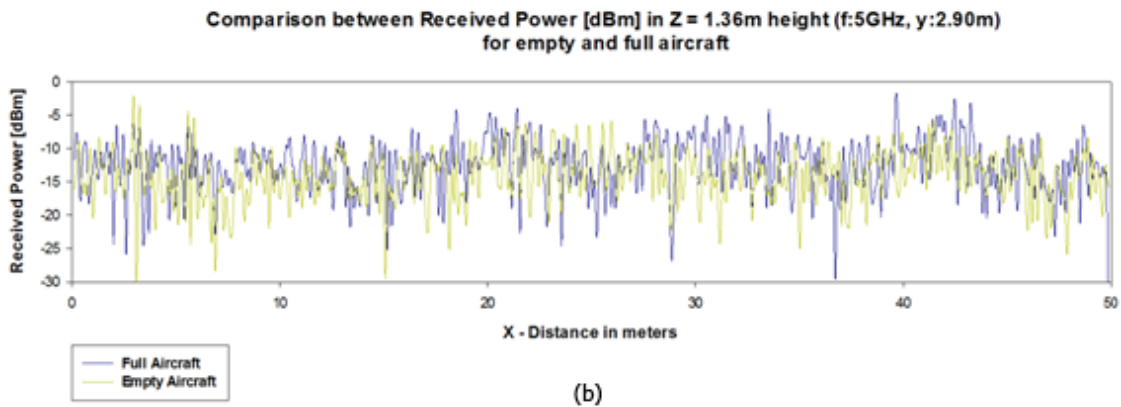
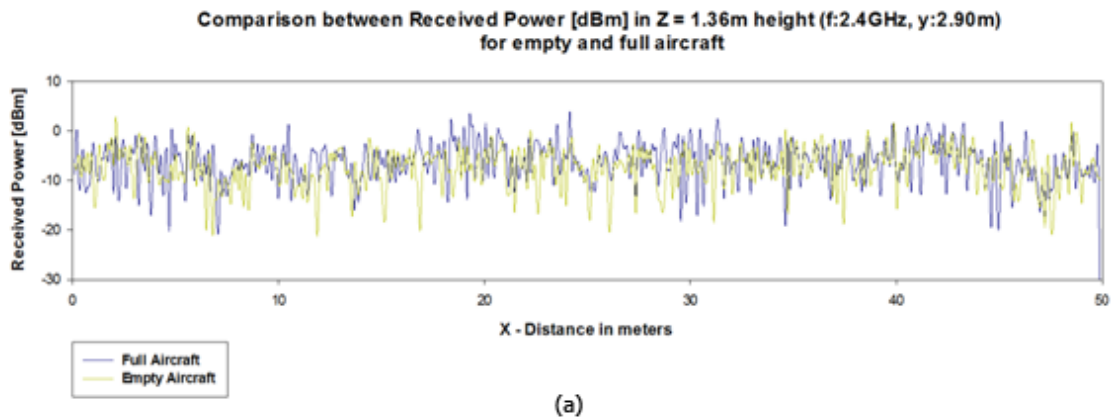


Figure 13 Comparison among the estimation of received power for Z=1.36m and Y=2.90m using 2.4GHz (a) and 5GHz (b) in empty and full aircraft

5. Impact of Multipath Propagation in the Aircraft Cabin

The difference among full and empty aircraft can be derived by observation of Power Delay estimations (Figure 14) where the power of the equivalent rays that cross one point for a given time period is depicted. Random seat side points for H1 and H2 have been chosen for those estimations. The aircraft cabin is mainly composed of metal giving rise to a very reflective environment and a high level of reflections are produced, increasing the probability that two or more rays cross the same observation point. When a ray crosses an absorptive object like a passenger seat a considerable amount of electromagnetic energy is lost and the number of the rays which can reach a point in space is decreased. In this sense delay spread is increased when the airplane is empty due to the fact that multi-path components are higher and some rays will be received later than in a full aircraft scenario.

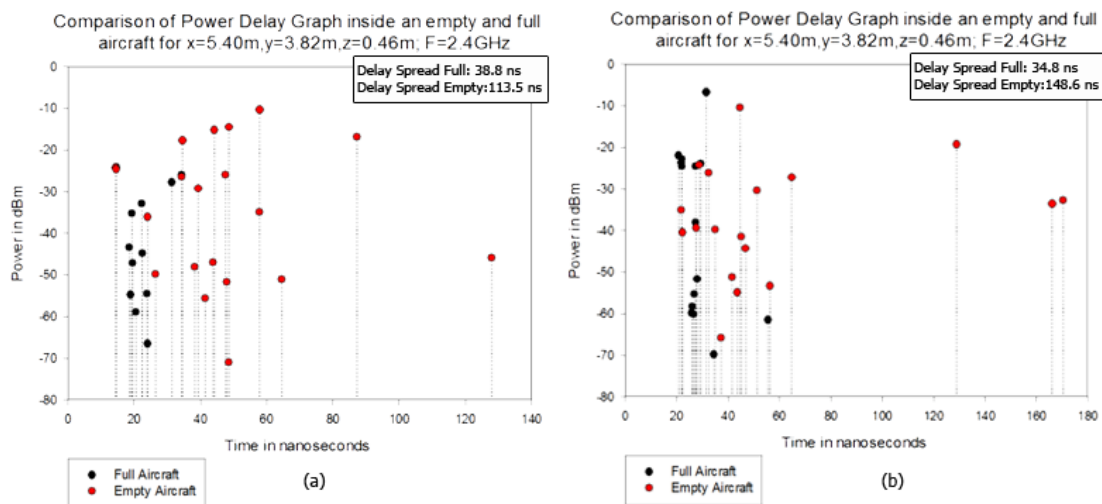


Figure 14 Comparison between power delay estimation for two seat side random points in H1(a) and H2(b) in full and empty aircraft(2.4GHZ).

In Figure 15 and Figure 16 the comparison between power delay distributions in full and empty aircraft is depicted for 5GHz and 900 MHz. As expected, higher level of power is received with lower frequencies but the elapsed times of ray arrivals are increased.

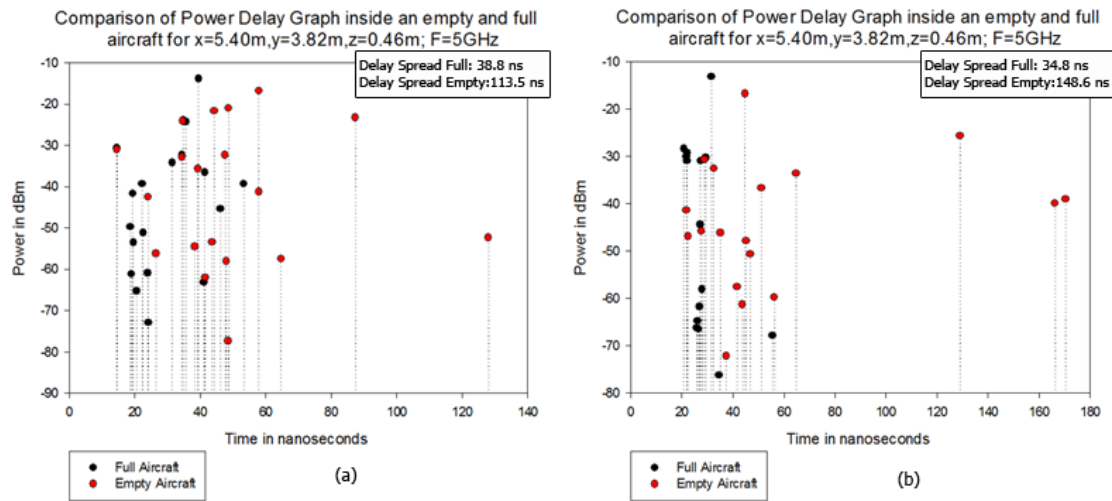


Figure 15 Comparison between power delay estimation for two seat side random points in H1(a) and H2(b) in full and empty aircraft(5GHz).

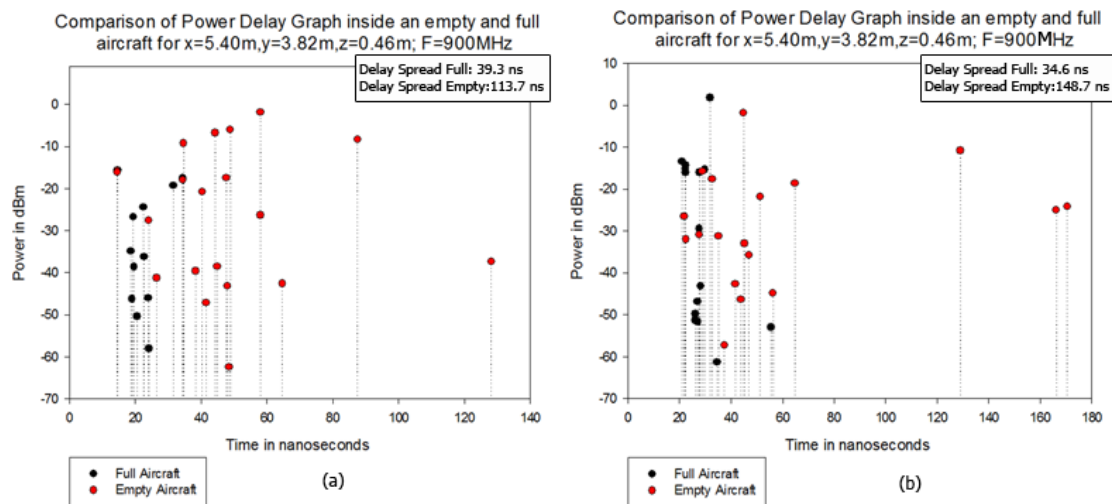


Figure 16 Comparison between power delay estimation for two seat side random points in H1(a) and H2(b) in full and empty aircraft(900MHz).

Delay spread is depicted in Figure 17 for the same two XY planes in full and empty aircraft. In those graphs the mentioned difference among full and empty aircraft is more noticeable, given by the absorption within the aircraft cabin.

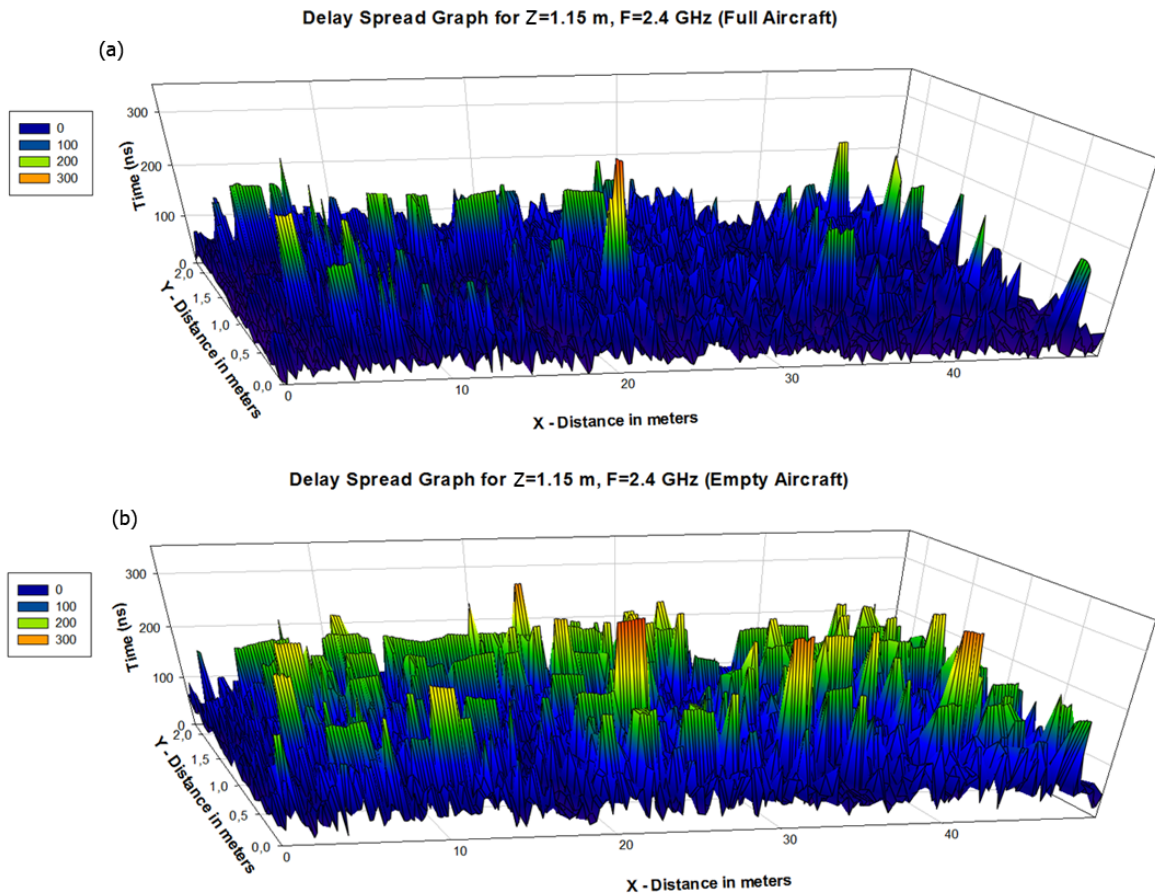


Figure 17 Estimation of delay spread inside full(a) and empty(b) aircraft in H2 (2.4GHz).

In Figure 18 the differences among the three frequencies delay spread is depicted. As it can be seen, there is a strong dependence of multipath components with the observation point, given by the inherent complexity in the morphology of the airplane environment. Moreover, comparison between the full aircraft and the empty scenario (i.e., no seats) shows that absorption effects in the full scenario modify the overall time distribution of the received field components. Therefore, radioplanning tasks within the aircraft cabin require the consideration of elements such as seats or baggage compartments in order to fully account for propagation losses and adequately deploy the on board antenna systems.

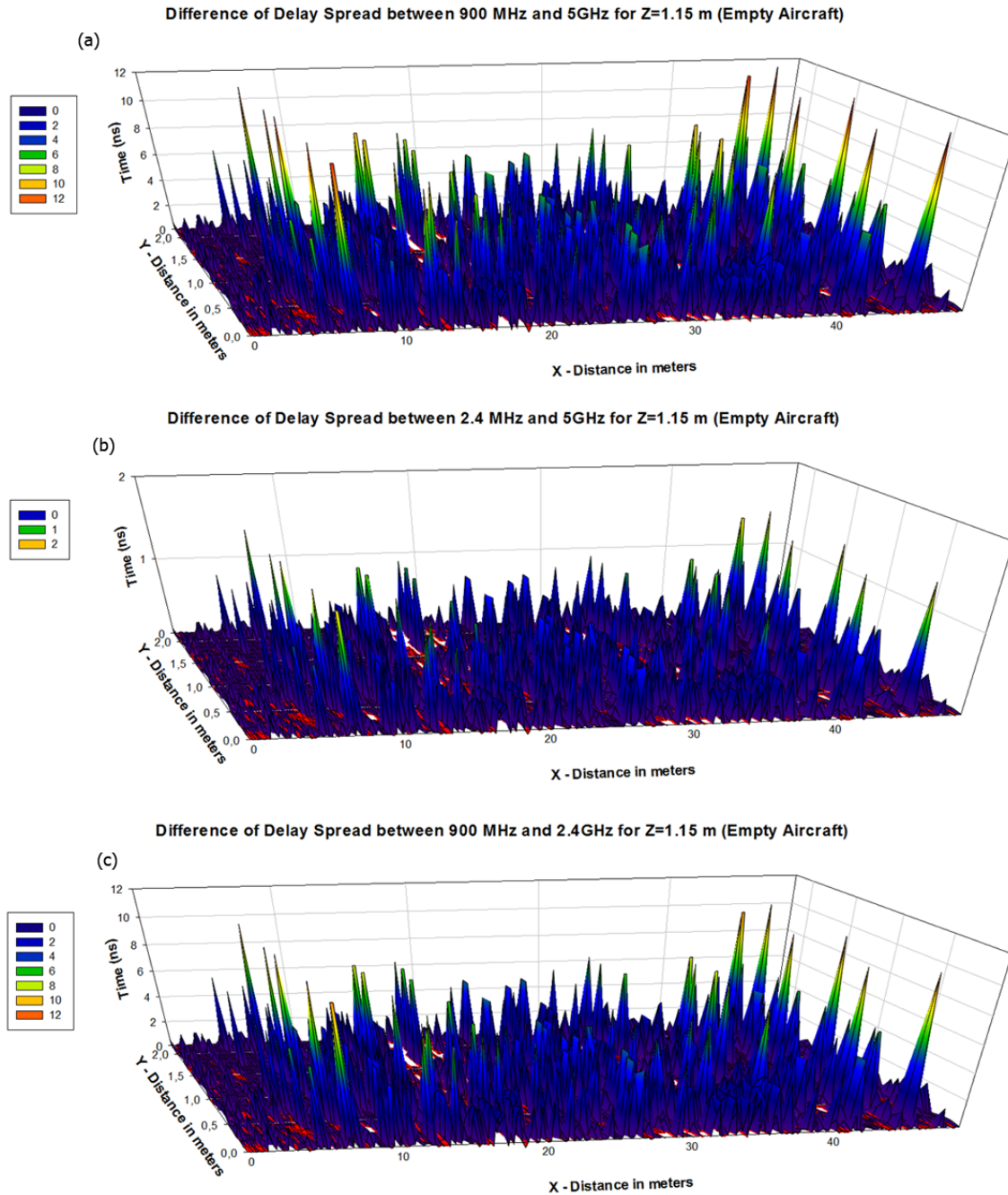


Figure 18 Difference between the delay spread estimated for three frequencies, 900MHz vs 5GHz (a), 2.4GHz vs 5GHz(b) and 900MHz vs 2.4GHz(c).

6. Conclusions

In this work, the characterization of wireless propagation in the main cabin of a commercial aircraft is analyzed. By means of in house implemented 3D ray launching code, estimation of radiopropagation losses as well as power delay profiles and power delay spread are obtained for the complete volume of a two deck Airbus A-380 aircraft. The simulation results have been obtained for different frequencies of

operation (900MHz, 2.4GHz and 5GHz) in order to consider the use of multiple spectrum allocated systems, mainly on board WLANs and Wireless Sensor Networks. Topology as well as morphology of the main cabin play a relevant role in the estimation of radiopropagation losses and hence, on the final radioplanning results. Complete morphological details, such as passenger seats, overhead luggage compartments, bathrooms and access stairs has been considered and their impact on multipath components has been estimated by comparing with an empty cabin. The use of deterministic simulation techniques such as 3D ray launching and the analysis of spatial power distribution as well as time dependent characteristics can aid in the deployment strategy of on board wireless systems, in order to minimize total interference, increase system performance and reduce power consumption.

7. References

- [1] A.R. Lopez, "GPS Landing System Reference Antenna", *IEEE Antennas and Propagation Magazine*, vol. 52, issue 1, pp. 104-113, 2010.
- [2] M. S. Reese¹, C. A. Balanis, C. R. Birtcher, G. C. Barber, "Modeling and Simulation of a Helicopter-Mounted SATCOM Antenna Array", *IEEE Antennas and Propagation Magazine*, vol. 53, no. 2, 2011.
- [3] G.W. Swenson Jr, "Radio Sociology", *IEEE Antennas and Propagation Magazine*, vol. 38, issue 2, pp. 45-47, 1996.
- [4] Y. Rahmat-Samii, K. S. Kona, M. Manteghi, S. Yueh, W. J. Wilson, S. Dinardo, D. Hunter, "A novel lightweight dual-frequency dual-polarized sixteen-element stacked patch microstrip array antenna for soil-moisture and sea-surface-salinity missions", *IEEE Antennas and Propagation Magazine*, vol. 48, issue 6, pp. 33-46, 2006.
- [5] J. Pinto, G. M. Lewis, J. A. Lord, R.A. Lewis, B. H. Wright, "Wireless data transmission within an aircraft environment", *Proceedings of the Fourth European Conference on Antennas and Propagation (EuCAP)*, Barcelona, Spain, 12-16 April 2010.
- [6] R. A. Volesky, B. A. Kish, D. O. Creviston, J. W. Geitguy, M. Kikuchi, J. C. Vap, "Air-to-Air Evaluation of an Amplified 802.11b Network", *IEEE Aerospace Conference*, Big Sky, MT, USA, 1-8 March, 2008.
- [7] C. R. Smith, M. Goggans, "Radar target identification", *IEEE Antennas and Propagation Magazine*, vol. 35, issue 2, pp. 27-38, 1993.
- [8] A. S. Zahmati, X. Fernando, H. Kojori, "Emerging wireless applications in aerospace: Benefits, challenges, and existing methods", *4th Annual Canopus Fly by Wireless Workshop (FBW)*, Montreal, Canada, 14-17 June, 2011.
- [9] R. Burda, C. Wietfeld, "Multimedia over 802.15.4 and ZigBee Networks for Ambient Environment Control", *IEEE 65th Vehicular Technology Conference (VTC)*, Dublin, Ireland, 22-25 April, 2007.
- [10] Jian Luo, W. Keusgen, A. Kortke, M. Peter, "A Design Concept for a 60 GHz Wireless In-Flight Entertainment System", *IEEE 68th Vehicular Technology Conference (VTC)*, Calgary, Canada, 21-24 Sept., 2008.
- [11] V. Ziegler, B. Schulte, J. Sabater, S. Bovelli, J. Kunisch, K. Maulwurf, M. Martinez-Vazquez, C. Oikonomopoulos-Zachos, S. Glisic, M. Ehrig, E. Grass, "Broadband 57-64-GHz WLAN Communication System Integrated Into an Aircraft Cabin", *IEEE Transactions on Microwave Theory and Techniques*, vol. 60, issue 12, pp. 4209-4219, 2012.
- [12] V. Ziegler, B. Schulte, J. Sabater, S. Bovelli, J. Kunisch, K. Maulwurf, M. Martinez-Vazquez, C. Oikonomopoulos-Zachos, S. Glisic, M. Ehrig, E. Grass, "Aircraft cabin-integrated 57-64GHz WLAN communication system", *IEEE MTT-S International Microwave Symposium Digest (MTT)*, Montreal, Canada, 17-22 June, 2012.
- [13] L. M. L. Oliveira, J. J. P. C. Rodrigues, B. M. Macao, P. A. Nicolau, Liang Zhou, "A WSN solution for light aircraft pilot health monitoring", *IEEE Wireless Communications and Networking Conference (WCNC)*, Shanghai, China, 1-4 April, 2012.
- [14] A. Ameti, R. J. Fontana, E. J. Knight, E. Richley, "Ultra wideband technology for aircraft wireless intercommunications systems (AWICS) design", *IEEE Aerospace and Electronic Systems Magazine*, vol. 19, issue 7, pp. 14-18, 2004.
- [15] P. Kopyt, "A 5.8 GHz RFID-based data transmission system as an energy efficient solution for on-board monitoring", *18th International Conference on Microwave Radar and Wireless Communications (MIKON)*, Vilnius, Lithuania, 14-16 June, 2010.

- [16] Lin Li, Jingsong Xie, O. M. Ramahi, M. Pecht, B. Donham, "Airborne operation of portable electronic devices", *IEEE Antennas and Propagation Magazine*, vol. 44, issue 4, pp. 30-39, 2002.
- [17] H. Hashemi, "The indoor radio propagation channel", *Proc. IEE*, 81, pp. 943-968, 1993.
- [18] J. Fink, N. Michael, A. Kushleyev, V. Kumar, "Experimental characterization of radio signal propagation in indoor environments with application to estimation and control", *Intelligent Robots and Systems (IROS)*, St. Louis, MO, USA, 2009.
- [19] J. M. Hernando, "Transmisión por Radio", 5th Ed.; Ed. Universitaria Ramón Areces: Madrid, Spain, 2008.
- [20] D.C.O'Brien, G.E.Faulkner, S.Zikic, N.P.Schmitt, "High data-rate optical wireless communications in passenger aircraft: Measurements and simulations", *6th International Symposium on Communication Systems, Networks and Digital Signal Processing (CNSDSP)*, Graz, Austria, 2008.
- [21] D. Marinos, C. Aidinis, C. Vassilopoulos, P. Kouros, N. Schmitt, T. Pistner, J. Schalk, J. Klaue, "Performance analysis of modulation schemes for wireless optical in-cabin aircraft networks", *International Symposium in Information Technology (ITSim)*, vol. 3, Kuala Lumpur, Malaysia, 15-17 June, 2010.
- [22] D. Marinos, C. Aidinis, N. Schmitt, J.Klaue, J. Schalk, T. Pistner, P. Kouros, "Wireless optical OFDM implementation for aircraft cabin communication links", *5th IEEE International Symposium on Wireless Pervasive Computing (ISWPC)*, Modena, Italy, 5-7 May, 2010.
- [23] S. Dimitrov, R. Mesleh, H. Haas, M. Cappitelli, M. Olbert, E. Bassow, "On the SIR of a Cellular Infrared Optical Wireless System for an Aircraft", *IEEE Journal on Selected Areas in Communications*, vol. 27, no. 9, 2009.
- [24] M. E. Yousefi, S. M. Idrus, C. H. Lee, M. Arsat, A. S. M. Supa'at, N. M. Safri, "Indoor free space optical communications for aircraft passenger cabin", *4th International Conference on Modeling, Simulation and Applied Optimization (ICMSAO)*, Kuala Lumpur, Malaysia, 19-21 April, 2011.
- [25] M. Peter, W. Keusgen, A. Kortke, M. Schirmacher, "Measurement and Analysis of the 60 GHz In-Vehicular Broadband Radio Channel", *IEEE 66th Vehicular Technology Conference (VTC)*, Baltimore, MD, USA, Sept. 30 2007-Oct. 3, 2007.
- [26] D. W. Matolak, A. Chandrasekaran, "Aircraft intra-vehicular channel characterization in the 5 GHz band", *Integrated Communications, Navigation and Surveillance Conference (ICNS)*, Bethesda, MD, USA, 5-7 May, 2008.
- [27] N. Moraitis, P. Constantinou, "Radio Channel Measurements and Characterization inside Aircrafts for In-Cabin Wireless Networks", *IEEE 68th Vehicular Technology Conference (VTC)*, Calgary, Canada, 21-24 Sept. 2008.
- [28] A. Skrebtsov, A. Burnic, Dong Xu, A. Waadt, P. Jung, "UWB applications in public transport", *International Conference on Communications, Computing and Control Applications (CCCA)*, Hammamet, Tunisia, 3-5 March, 2011.
- [29] N. R. Diaz, J. E. J. Esquitino, "Wideband channel characterization for wireless communications inside a short haul aircraft", *IEEE 59th Vehicular Technology Conference (VTC)*, vol.1, 17-19 May, 2004.
- [30] Zhenghui Li, Fengyu Luan, Yan Zhang, Limin Xiao, Lianfen Huang, Shidong Zhou, Xibin Xu, Jing Wang, "Capacity and spatial correlation measurements for wideband distributed MIMO channel in aircraft cabin environment", *IEEE Wireless Communications and Networking Conference (WCNC)*, Shanghai, China, 1-4 April, 2012.
- [31] R. S. A. Peruvemba, C. Furse, "Enabling wireless communication in aircraft using multiple antenna system", *IEEE Antennas and Propagation Society International Symposium (APSURSI)*, Charleston, SC, USA, 1-5 June, 2009.
- [32] Wei-Jiang Zhao, Er-Ping Li, Viet Phuong Bui, Bing-Fang Wang, "Modeling of transmission characterisation in aircraft cabins with a hybrid technique", *IEEE International Symposium on Antennas and Propagation (APSURSI)*, Spokane, WA, USA, 3-8 July, 2011.
- [33] M. Jafri, J. Ely, L. Vahala, "Fuzzification of electromagnetic interference patterns onboard commercial airliners due to wireless technology", *IEEE Antennas and Propagation Society International Symposium*, 20-25 June, 2004.
- [34] V. Koudelka, Z. Raida, P. Tobola, "Simple Electromagnetic Modeling of Small Airplanes: Neural Network Approach", *Radioengineering*, vol. 18, no. 1, April 2009.
- [35] G. Hankins, L. Vahala, J. H. Beggs, "Electromagnetic propagation prediction inside aircraft cabins", *IEEE Antennas and Propagation Society International Symposium*, 20-25 June, 2004.
- [36] G. Hankins, L. Vahala, J. H. Beggs, "802.11ab propagation prediction inside a B777", *IEEE/ACES International Conference on Wireless Communications and Applied Computational Electromagnetics*, 3-7 April, 2005.
- [37] E. Perrin, F. Tristant, S. Gouverneur, R. Fayat, C. Guiffaut, A. Reineix, J-P. Moreau, "Study of electric field radiated by WiFi sources inside an aircraft - 3D computations and real tests", *International Symposium on Electromagnetic Compatibility (EMC) Europe*, Hamburg, Germany, 8-12 Sept., 2008.
- [38] T. Hikage, T. Nojima, M. Omiya, K. Yamamoto, "Numerical analysis of electromagnetic field distributions in a typical aircraft", *International Symposium on Electromagnetic Compatibility (EMC) Europe*, Hamburg, Germany, 8-12 Sept., 2008.
- [39] M. F. Iskander, Zhengqing Yun, "Propagation prediction models for wireless communication systems", *IEEE Transactions on Microwave Theory and Techniques*, vol. 50, issue 3, pp. 662-673, 2002.
- [40] K. Chetcuti, C. J. Debono, R. A. Farrugia, S. Bruillot, "Wireless propagation modelling inside a business jet", *IEEE EUROCON*, St. Petersburg, Russia, 18-23 May, 2009.
- [41] C. J. Debono, K. Chetcuti, S. Bruillot, "802.11a channel parameters characterization on board a business jet", *IEEE Aerospace conference*, Big Sky, MT, USA, 7-14 March, 2009.

- [42] C. De Raffaele, C. J. Debono, "Modeling of the electromagnetic interference map generated by 3G systems inside small aircraft", *International Conference on Wireless Communications and Signal Processing (WCSP)*, Suzhou, China, 21-23 Oct., 2010.
- [43] Chao Zhang, Junzhou Yu, "Real-time aircraft cabin channel modeling", *IEEE 13th International Conference on Communication Technology (ICCT)*, Jinan, China, 25-28 Sept., 2011.
- [44] C. De Raffaele, C. J. Debono, A. Muscat, "Simulating electromagnetic field inside small aircraft from wireless camera equipment", *Antennas and Propagation Conference (LAPC)*, Loughborough, UK, 12-13 Nov., 2012.
- [45] J. R. Nagel, A. M. Richards, S. Anantharayanan, C. M. Furse, "Measured Multi-User MIMO Capacity in Aircraft", *IEEE Antennas and Propagation Magazine*, vol. 52, no.4, August 2010.
- [46] C. J. Debono, R. A. Farrugia, "Optimization of the UMTS Network Radio Coverage On-board an Aircraft", *IEEE Aerospace Conference*, Big Sky, MT, USA, 1-8 March, 2008.
- [47] K. Chetcuti, C. J. Debono, S. Bruillot, "The effect of human shadowing on RF signal strengths of IEEE 802.11a systems on board business jets", *IEEE Aerospace Conference*, Big Sky, MT, USA, 6-13 March, 2010.
- [48] C. De Raffaele, C. J. Debono, A. Muscat, "Modeling electromagnetic interference generated by a WLAN system onboard commercial aircraft", *15th IEEE Mediterranean Electrotechnical Conference MELECON*, Valletta, Malta, 26-28 April, 2010.
- [49] C. De Raffaele, C. J. Debono, A. Muscat, "Small aircraft cockpit electromagnetic interference due to UMTS signal propagation", *IEEE International Conference on Wireless Information Technology and Systems (ICWITS)*, Honolulu, HI, USA, Aug. 28-Sept. 3, 2010.
- [50] B. Choudhury, H. Singh, J. P. Bommer, R. M. Jha, "RF Field Mapping Inside a Large Passenger-Aircraft Cabin Using a Reflected Ray-Tracing Algorithm", *IEEE Antennas and Propagation Magazine*, vol. 55, no. 1, February 2013.
- [51] L. Azpilicueta, F. Falcone, J. J. Astráin, J. Villadangos, I. J. García Zuazola, H. Landaluce, I. Angulo, A. Perallos, "Measurement and modeling of a UHF-RFID system in a metallic closed vehicle", *Microwave and Optical Technology Letters*, vol. 54, issue 9, pp. 2126-2130, 2012.
- [52] J. A. Nazábal, P. L. Iturri, L. Azpilicueta, F. Falcone, C. Fernández-Valdivielso, "Performance Analysis of IEEE 802.15.4 Compliant Wireless Devices for Heterogeneous Indoor Home Automation Environments", *International Journal of Antennas and Propagation*, Hindawi Publishing Corporation, Article ID 176383, 2012.
- [53] E. Aguirre, J. Arpón, L. Azpilicueta, S. de Miguel, V. Ramos, F. Falcone, "Evaluation of electromagnetic dosimetry of wireless systems in complex indoor scenarios with human body interaction", *Progress In Electromagnetics Research B*, vol. 43, pp. 189-209, 2012.
- [54] P. L. Iturri, J. A. Nazabal, L. Azpilicueta, P. Rodriguez, M. Beruete, C. Fernandez-Valdivielso, F. Falcone, "Impact of High Power Interference Sources in Planning and Deployment of Wireless Sensor Networks and Devices in the 2.4 GHz Frequency Band in Heterogeneous Environments", *Sensors*, vol. 12, issue 11, pp. 15689-15708, 2012.
- [55] Jianhua Liu, I. Demirkiran, T. Yang, A. Helfrick, "Feasibility study of IEEE 802.15.4 for aerospace wireless sensor networks", *IEEE/AIAA 28th Digital Avionics Systems Conference*, Orlando, FL, USA, 23-29 Oct., 2009.
- [56] H. D. Hristov, "Fresnel Zones in Wireless links, zone plate lenses and antennas", s.l., Artech House, 2000.
- [57] R. J. Luebbers, "A Heuristic UTD Slope Diffraction Coefficient for Rough Lossy Wedges", *IEEE Transactions on Antennas and Propagation*, vol. 37, pp. 206-211, 1989.
- [58] W. Dong, G. Liu, L. Yu, H. Ding, J. Zhang, "Channel properties of indoor part for high-speed train based on wideband channel measurement", *Communications and Networking in China (CHINACOM)*, 2010, 5th International ICST Conference.
- [59] K. Siwiak, "Radiowave propagation and antennas for personal communications", Artech House, Inc., 1998.